

X-Ray Flashes on Helium Novae

MARIKO KATO ¹ AND IZUMI HACHISU ²

¹*Department of Astronomy, Keio University, Hiyoshi, Kouhoku-ku, Yokohama 223-8521, Japan*

²*Department of Earth Science and Astronomy, College of Arts and Sciences, The University of Tokyo, 3-8-1 Komaba, Meguro-ku, Tokyo 153-8902, Japan*

ABSTRACT

A helium nova occurs on a white dwarf (WD) accreting hydrogen-deficient matter from a helium star companion. When the mass of a helium envelope on the WD reaches a critical value, unstable helium burning ignites to trigger a nova outburst. A bright soft X-ray phase appears in an early outbursting phase of a helium nova before it optically rises toward maximum. Such an X-ray bright phase is called the X-ray flash. We present theoretical light curves of X-ray flashes for 1.0, 1.2, and 1.35 M_{\odot} helium novae with mass accretion rates of $(1.6 - 7.5) \times 10^{-7} M_{\odot} \text{ yr}^{-1}$. Long durations of the X-ray flashes (100 days to 10 years) and high X-ray luminosities ($\sim 10^{38} \text{ erg s}^{-1}$) indicate that X-ray flashes are detectable as a new type of X-ray transient or persistent X-ray sources. An X-ray flash is a precursor of optical brightening, so that the detection of X-ray flashes on helium novae enables us to plan arranged observation for optical premaximum phases that have been one of the frontiers of nova study. We found a candidate object of helium-burning X-ray flash from literature on extragalactic X-ray surveys. This X-ray transient source is consistent with our X-ray flash model of a 1.35 M_{\odot} WD.

Keywords: novae, cataclysmic variables — stars: winds — stars: X-ray — white dwarfs

1. INTRODUCTION

A helium nova is a rare phenomenon triggered by unstable helium nuclear burning on a white dwarf (WD) (Taam 1980; Iben & Tutukov 1994; Cassisi et al. 1998; Cui et al. 2018; Kato et al. 2018). The first identified helium nova is the Galactic nova V445 Pup (Ashok & Banerjee 2003; Kato & Hachisu 2003; Iijima & Nakanishi 2008). Its outburst was discovered on UT 2000 December 30 (Kato & Kanatsu 2000).

The helium nova as an optical phenomenon was theoretically predicted by Kato et al. (1989): they pointed out two cases of helium accretion; (1) the WD accretes helium from a helium star companion, and (2) the WD is in a steady hydrogen burning, in which the accreted hydrogen is burned into helium at the same rate as the accretion. The third case occurs on a mass increasing WD. (3) A helium shell flash eventually occurs after a number of successive hydrogen shell flashes and a certain amount of helium accumulates underneath the hy-

drogen burning zone (Cassisi et al. 1998; Idan et al. 2013; Kato et al. 2017).

Long term evolutions of helium accreting WDs are also interested in binary evolution models toward a Type Ia supernova (Ablimit 2022; Wang et al. 2009, 2017; Wong & Schwab 2019; Kemp et al. 2021; Kool et al. 2023; Maguire et al. 2023).

1.1. Evolutions of helium novae in the HR diagram

Figure 1 shows one cycle helium shell flashes on a 1.2 M_{\odot} WD with the mass accretion rate of $\dot{M}_{\text{acc}} = 1.6, 3, \text{ and } 6 \times 10^{-7} M_{\odot} \text{ yr}^{-1}$, the data of which are taken from Kato et al. (2018). Each model cycle shows a loop in the HR diagram; it evolves anti-clockwise from the bottom (quiescent phase), early X-ray bright phase (X-ray flash), wind phase (optically bright phase), supersoft X-ray source (SSS) phase, and it finally becomes dark (post SSS phase).

When the envelope expands until the epoch denoted by a small open circle, optically thick winds begin to emerge from the photosphere. Because the winds are accelerated deep inside the photosphere, we call them the optically thick winds (e.g., Kato & Hachisu 1994). The wind phase begins at the small open circle and ends

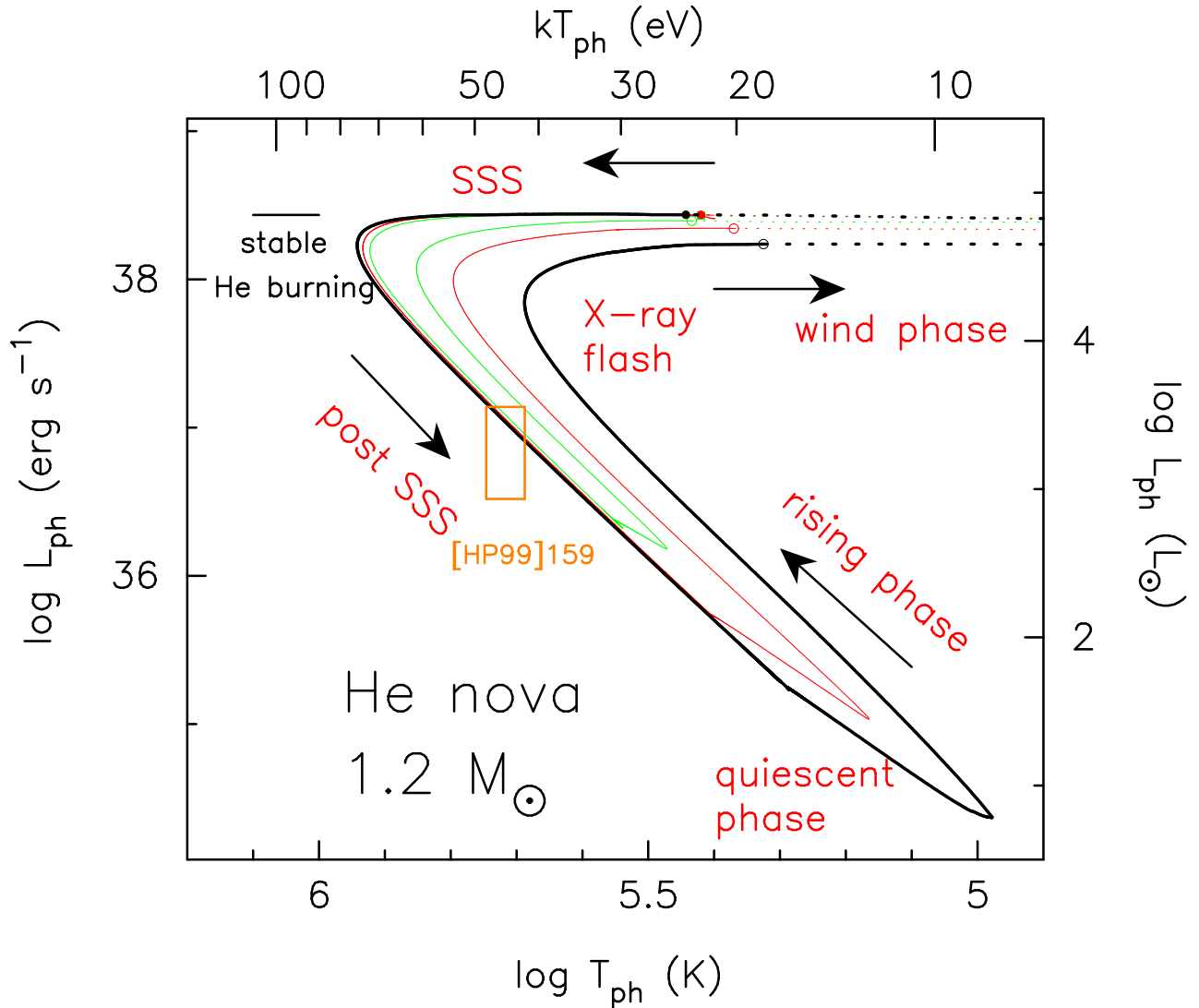


Figure 1. The HR diagram for $1.2 M_{\odot}$ helium nova models with the mass accretion rate of $\dot{M}_{\text{acc}} = 1.6 \times 10^{-7} M_{\odot} \text{ yr}^{-1}$ (black line), $3 \times 10^{-7} M_{\odot} \text{ yr}^{-1}$ (thin red line), and $6 \times 10^{-7} M_{\odot} \text{ yr}^{-1}$ (thin green line). The original data are taken from Kato et al. (2018). The photospheric temperature is denoted by T (K) or kT (eV), where T is the temperature in units of Kelvin and k is the Boltzmann constant. Each arrow indicates the direction of evolution. Optically thick winds start at the small open circles and ends at the filled circles on each track. The dotted lines correspond to their wind phases. The orange square shows the range of temperature and brightness for the LMC supersoft X-ray source [HP99]159 estimated by Greiner et al. (2023). The short horizontal bar indicates the luminosity of a $1.2 M_{\odot}$ WD in stable helium burning for the temperature range of [HP99]159.

at the filled circle on each track. In the upper leftward evolution of each track, the envelope mass decreases with time owing to both nuclear burning and wind mass loss. After the wind stops, the envelope mass decreases owing only to nuclear burning. In the SSS phase, the WD photosphere emits supersoft X-rays. After that, helium nuclear burning extinguishes and the WD becomes dark. The three model tracks are located almost on the same line in the SSS phase because each helium envelope reaches the same thermal and hydrostatic balance. These physical properties are essentially the

same as those in hydrogen shell flashes (Kovetz 1998; Denissenkov et al. 2013; Kato et al. 2022a, 2024).

The short horizontal bar in Figure 1 corresponds to the luminosity of a $1.2 M_{\odot}$ WD in the steady helium burning $\log L_{\text{ph}}/L_{\odot} = 4.85$. If the WD accretes mass at the same rate as the mass-decreasing rate owing to helium burning, the envelope mass is unchanged and the photospheric temperature is also the same. Thus, the WD stays at the same position in the HR diagram. Such WDs are observationally classified as persistent X-ray sources (Kahabka & van den Heuvel 1997). The mass accretion rates for stable he-

lium burning have been obtained for various WD masses (Kawai et al. 1988; Iben & Tutukov 1989; Wang et al. 2015; Brooks et al. 2016; Wang et al. 2017; Kato et al. 2018).

1.2. *First helium nova: V445 Puppis*

The spectral feature of V445 Pup resembles those of classical slow novae except very strong emission lines of carbon and the absence of hydrogen (Iijima & Nakanishi 2008). The optical light curve declines very slowly during 200 days followed by dust blackout, and has not recovered yet. We have no report for X-ray detections of V445 Pup.¹ Probably a supersoft X-ray source (SSS) phase had been obscured by a thick dust layer. Thus, we have no information on the date when the helium shell burning ended.

Kato et al. (2008) calculated theoretical light curve models for V445 Pup based on the steady-state approximation, and concluded that the WD is as massive as $\gtrsim 1.35 M_{\odot}$. Such a massive WD with a helium star companion has been discussed in relation to Type Ia supernova progenitors (e.g., Banerjee et al. 2003; Jacobson-Galán et al. 2019; Kool et al. 2023; Maguire et al. 2023).

1.3. *Second helium nova: LMC [HP99]159*

The LMC supersoft X-ray source [HP99]159 is the second candidate for a helium nova. Greiner et al. (2023) presented detailed observational summary for [HP99]159. The optical spectrum of [HP99]159 is hydrogen-free, so they concluded that the companion is a helium star. This object has been observed with several X-ray satellites since the Einstein satellite in 1979, followed by EXOSAT, ROSAT, XMM-Newton, Swift, and SRG/eROSITA. Greiner et al. (2023) estimated the luminosity and temperature of [HP99]159 as shown in Figure 1. They interpreted this object as a steady helium-shell burning source, with a suggestion of a $1.2 M_{\odot}$ WD, although the X-ray flux is two orders of magnitude smaller than the luminosity of a steady helium-shell burning WD.

Note that nuclear burning is stable in the upper leftward evolution branch (horizontal part) in the HR diagram (Figure 1), but unstable in the following downward evolution branch (post-SSS phase) (Sienkiewicz 1975, 1980; Kawai et al. 1988; Nomoto et al. 2007). When the WD evolves into the lower branch, nuclear burning

extinguishes and then the WD cools downward on the track.

Greiner et al. (2023) interpreted the X-ray luminosity of [HP99]159 as a steady helium-shell burning on a WD and claimed that such a low luminosity is possible when the WD is rotating addressing Yoon et al. (2004)'s numerical work. However, Yoon et al. showed that, while rotation does enhance stability, the accretion rates required to explain LMC [HP99]159 as a steady-state supersoft X-ray source are still too low to remain stable even in favorable rotation rates. This paper rather presents counterargument against such a low-luminosity steady helium-shell burning. Thus, it is unlikely that [HP99]159 is a steady helium shell burning object, at least, from the theoretical point of view.

Kato et al. (2023) presented another interpretation for this faint X-ray flux as a post-SSS phase of a helium nova outburst. Kato et al. calculated post-SSS light curves based on the helium nova models, and showed that a $\sim 1.2 M_{\odot}$ helium nova has a long decay phase consistent with the X-ray observation of [HP99]159 since 1980. Unfortunately, its optical outburst has not been reported. In any case, the presence of a binary with a helium donor star like [HP99]159 suggests that helium accreting WDs are rather abundant.

1.4. *Search for X-ray flashes on helium novae*

The X-ray observation of novae have provided useful information for us to advance quantitative study of nova outbursts. In particular, the SSS phase has been a useful tool in determining the WD mass (e.g., Sala & Hernanz 2005; Hachisu & Kato 2010; Wolf et al. 2013a; Kato & Hachisu 2020). In helium novae, however, the SSS phase may be difficult to observe because a thick dust layer forms soon after the optical maximum, like in V445 Pup. Extremely strong carbon emission lines observed in V445 Pup suggest that massive carbonaceous dust forms in helium novae because carbon is a main nuclear product of helium burning. On the other hand, an X-ray flash before optical brightening is not obscured by dust because of unpolluted environment. Thus, the detection of X-ray flashes is a unique tool for quantitative study of helium novae with X-rays.

In this work, we present theoretical light curves of X-ray flashes for helium novae with various WD masses and mass accretion rates. This paper is organized as follows. Section 2 briefly describes our numerical method and presents results for the X-ray flashes of helium novae. In Section 3, we present a candidate object of helium-burning X-ray flashes. Concluding remarks follow in Section 4.

¹No record of V445 Pup in the ROSAT all sky survey source catalog: period between June 1990 and August 1991. www.mpe.mpg.de/ROSAT/2RXS

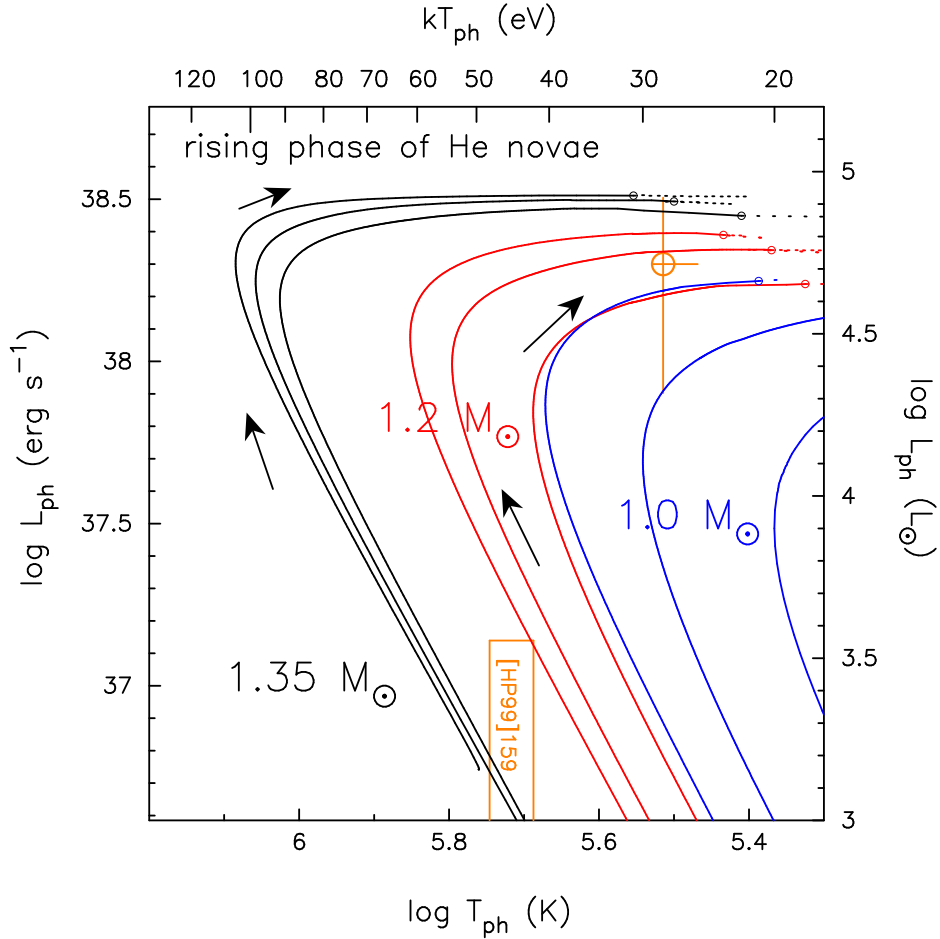


Figure 2. Close up view of rising phases of helium novae in the HR diagram. From upper to lower, the three black lines indicate $1.35 M_{\odot}$ WD models with mass accretion rates of $\dot{M}_{\text{acc}} = (7.5, 3.0, 1.6) \times 10^{-7} M_{\odot} \text{ yr}^{-1}$, three red lines $1.2 M_{\odot}$ WD models with $(6.0, 3.0, 1.6) \times 10^{-7} M_{\odot} \text{ yr}^{-1}$, and three blue lines $1.0 M_{\odot}$ WD models with $(6.0, 3.0, 1.6) \times 10^{-7} M_{\odot} \text{ yr}^{-1}$. Each arrow indicates the direction of evolution. Model parameters are summarized in Table 1. Optically thick winds start at the small open circles on each track. The dotted lines corresponds to the wind phase. For comparison, we add the position of an X-ray flash of the classical nova YZ Ret (König et al. 2022), which was not a helium nova but originated from a hydrogen shell flash (orange circle with error bars). The orange square shows the range of temperature and brightness for the LMC supersoft X-ray source [HP99]159 estimated by Greiner et al. (2023).

Table 1. Model parameters of He shell flashes

Model	M_{WD} (M_{\odot})	\dot{M}_{acc} ($M_{\odot} \text{ yr}^{-1}$)	P_{rec} (yr)	M_{acc} (M_{\odot})	$L_{\text{nuc}}^{\text{max}}$ (L_{\odot})	$\log L_{X>0.2}^{\text{peak}}$ (L_{\odot})	$\log L_{X>0.3}^{\text{peak}}$ (L_{\odot})
M10.6	1.0	6.0×10^{-7}	1270	7.4×10^{-4}	2.5×10^7	3.81	3.12
M10.3	1.0	3.0×10^{-7}	7330	2.2×10^{-3}	6.2×10^9	3.18	2.15
M10.16	1.0	1.6×10^{-7}	31800	5.1×10^{-3}	2.6×10^{11}	2.00	0.24
M10.1	1.0	1.0×10^{-7}	74200	7.4×10^{-3}	1.5×10^{12}	0.41	-2.20
M12.6	1.2	6.0×10^{-7}	444	2.6×10^{-4}	7.1×10^7	4.37	4.00
M12.3	1.2	3.0×10^{-7}	1990	5.9×10^{-4}	3.3×10^9	4.20	3.75
M12.16	1.2	1.6×10^{-7}	9340	1.5×10^{-3}	2.5×10^{11}	3.83	3.18
M135.75	1.35	7.5×10^{-7}	34.1	2.5×10^{-5}	5.0×10^6	4.77	4.62
M135.3	1.35	3.0×10^{-7}	203	6.0×10^{-5}	5.0×10^8	4.72	4.54
M135.16	1.35	1.6×10^{-7}	743	1.2×10^{-4}	8.5×10^9	4.65	4.45

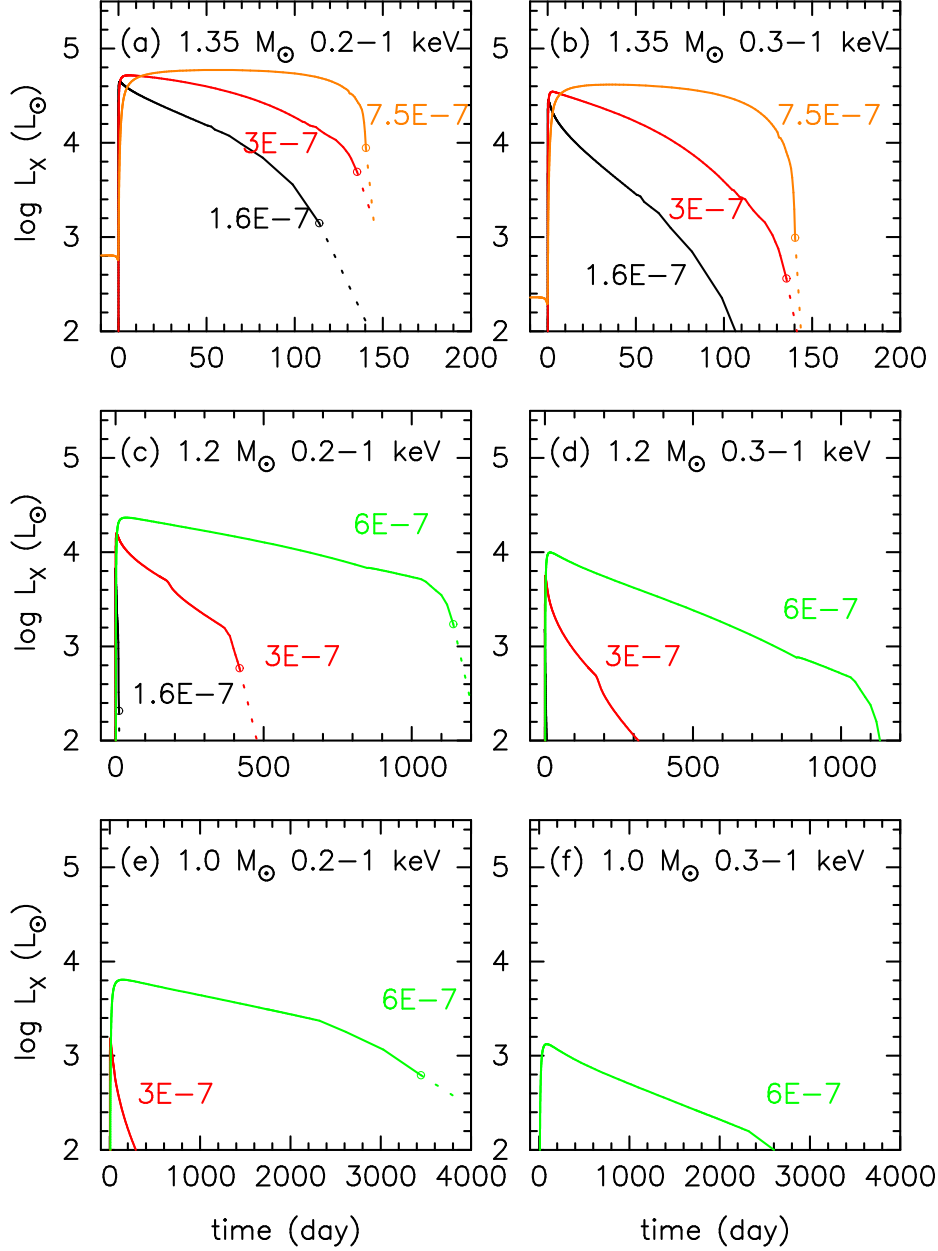


Figure 3. X-ray flash light curves of helium novae. The left column panels (a), (c), and (e) show the light curves for a 0.2–1.0 keV energy band, corresponding to the SRG/eROSITA instrument. The right column panels (b), (d), and (f) show a 0.3–1.0 keV energy band for the Swift/XRT. In the $1.0 M_\odot$ WD models, X-ray photons are very soft and make large difference between the two bands. To show that X-ray photons with $E_X > 1$ keV are negligible, we recalculated lines in panel (b) for the energy range of 0.3–10 keV. The lines are not changed within the line width. The open circles indicate the starting points of optically thick winds (Kato & Hachisu 1994). Once the winds start to emerge from the photosphere, we expect no significant X-ray flux owing to the self-absorption effect of the wind itself outside the photosphere.

2. MODEL CALCULATION OF X-RAY FLASHES

2.1. *X-ray flash light curves on helium novae*

We have calculated X-ray light curves based on the helium nova models obtained by Kato et al. (2018). These models are calculated with a Henyey type evolution code. The occurrence of an optically thick wind is detected by the condition BC1 in Kato & Hachisu (1994). We assumed helium-rich matter accretion of $X = 0.0$, $Y = 0.98$, and $Z = 0.02$.

Table 1 lists our model parameters. From left to right, model name, WD mass, mass accretion rate, recurrence period of helium nova outbursts, accreted mass, maximum nuclear energy generation rate, and the maximum X-ray luminosities at the photosphere for 0.2 – 1.0 keV and 0.3 – 1.0 keV energy band.

These mass-accretion rates are broadly consistent with the high mass-transfer rates calculated for Roche-lobe-filling helium stars (Kato et al. 2008; Brooks et al. 2016).

Figure 2 is a close-up view of the HR diagram that shows each helium nova model in Table 1, but only in the X-ray flash phase. For the same WD mass, e.g., $1.35 M_{\odot}$ WD, the track of the highest sampled accretion rate is located on the farthest upper-left side. As the accretion rate becomes smaller, the track moves to the lower-right side.

Figure 3 shows the X-ray light curves during the flash phase corresponding to the model in Figure 2. The left column panels show the 0.2 – 1.0 keV band fluxes, corresponding to the SRG/eROSITA instrument (e.g., König et al. 2022), while the right column panels are for the 0.3 – 1.0 keV band, corresponding to the Swift/XRT (e.g., Evans et al. 2009). As the X-rays are very soft, most of which are below 1.0 keV, the flux hardly changes even if we adopt another upper limit of > 1 keV. We recalculated light curves in Figure 3b for the energy range of 0.3 - 10 keV, but found no differences between the two different bands.

In each panel, a WD model with a higher mass-accretion rate evolves slowly, and the bright X-ray phase lasts longer. In a higher mass-accretion rate, the ignition mass is smaller, which results in a smaller pressure at the bottom of the envelope. Thus, the peak nuclear luminosity $L_{\text{nuc}}^{\text{max}}$ is smaller, as listed in Table 1. A smaller nuclear energy generation rate makes expansion slower in the X-ray flash phase where the evolution speed is governed by convective energy transport. Thus, the photospheric radius expands more slowly, and the decrease in the photospheric temperature is slower. This tendency

is the same as that in hydrogen shell flashes (hydrogen novae) as clearly discussed by Kato et al. (2024).

In the $1.35 M_{\odot}$ models, the X-ray phases last about 150 days for the both bands (Figure 3(a) and (b)). For less massive WDs, the evolutions are slower and the bright X-ray phase becomes much longer. The difference between the two bands becomes remarkable, especially in the $1.0 M_{\odot}$ WD models because the emitted supersoft X-rays are softer for lower photospheric temperatures, as shown in Figure 2.

2.2. *Comparison with X-ray flashes on hydrogen novae*

The classical nova YZ Reticuli is only the nova whose X-ray flash has been detected (König et al. 2022). It was observed by the eROSITA instrument on board Spectrum-Roentgen-Gamma (SRG) when it scanned the region of YZ Ret (König et al. 2022).

We plot the position of YZ Ret in the HR diagram (Figure 2). YZ Ret is a hydrogen nova, but it is located at a similar region to helium novae in the HR diagram. This clearly demonstrates that the X-ray flash is detectable also for a helium nova.

The X-ray flash of YZ Ret lasted very short of < 8 hr (König et al. 2022) and preceded the optical maximum by about 2 – 3 days. Such a brief duration and short preceding time to the optical maximum suggest a very massive WD of $M_{\text{WD}} \gtrsim 1.3 M_{\odot}$ (Kato et al. 2022b,c). Hachisu & Kato (2023) estimated the WD mass to be $1.33 M_{\odot}$ from their light curve analysis by comparing model light curves with multiwavelength observation.

The detection of the X-ray flash in YZ Ret gives a large impact to the study of novae. (1) The luminosity, temperature, and blackbody spectrum (König et al. 2022) are consistent with theoretical scenario that a nova expands in almost hydrostatically until an optically thick wind begins to blow (Hachisu & Kato 2022). (2) It is confirmed that no strong shock waves form at this very early stage.

Theoretically, X-ray flash light curves of helium novae should have similar properties to those in hydrogen novae except for their timescales (see, e.g., Kato et al. 2022b, for X-ray flash light curves of hydrogen novae). We encourage X-ray flash observations of helium novae.

3. HELIUM-BURNING X-RAY FLASHES AS A NEW TYPE OF TRANSIENT SOURCE

The X-ray flashes of helium novae could be detected as a new type of X-ray transient with the X-ray luminosity of $L_{\text{X}} \sim 10^{38}$ erg s $^{-1}$, because of their relatively longer durations (100 days to 10 yr), probably with no optical counterparts. We searched the literature of X-ray surveys for candidates of helium-burning X-ray flashes.

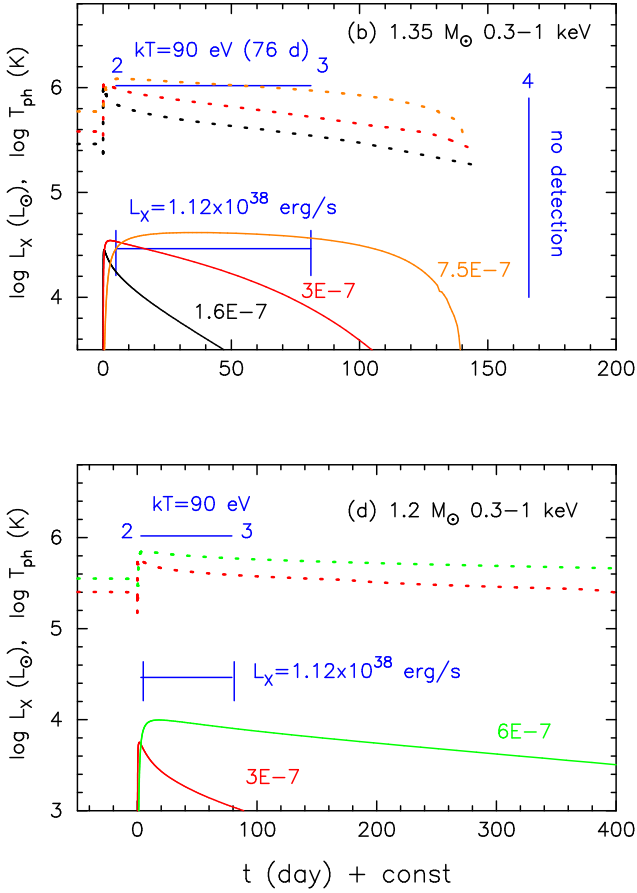


Figure 4. Same as Figure 3, but only panels (b) and (d) are shown with the temporal variation in the photospheric temperature (dotted line). The horizontal blue lines show the photospheric blackbody temperature of $kT_{\text{ph}} = 90$ eV and luminosity $L_X = 1.12 \times 10^{38} \text{ erg s}^{-1}$ with one σ range estimated for the X-ray source A6 in NGC 3379 (Brassington et al. 2012). This object is detected twice at epochs 2 and 3 (separated by 76 days), but not at epoch 4.

Brassington et al. (2008, 2012) reported 18 potential transient X-ray sources detected with Chandra in nearby early-type galaxies. Among them, the authors classified the X-ray source, A6 (Source No. 100 in Brassington et al. 2008) in NGC 3379, to be the SSS phase of a classical nova. The X-ray luminosity is $L_X = 1.12 \times 10^{38} \text{ erg s}^{-1}$ (0.3 - 8.3 keV) with a blackbody temperature of 90 eV with the hydrogen column density of $N_{\text{H}} = 2.8 \times 10^{20} \text{ cm}^{-2}$. The one σ range of L_X is $(0.62 - 1.67) \times 10^{38} \text{ erg s}^{-1}$. This source is detected twice with 76 days separation and did not detected 1805 days before the first detection, and 85 days after the second detection. No optical counterpart is detected with the limit of 26.4 mag.

It has been discussed that a blackbody fit does not always work well in the SSS phase of a nova outburst and results in implausible temperature and lumi-

nosity (e.g., Krautter et al. 1996; Henze et al. 2011; Osborne et al. 2011; Page et al. 2015), partly because the spectrum is strongly contaminated by absorption and emission lines. However, differently to SSS phases, X-ray flashes occur before massive mass ejection starts. Therefore, spectra of X-ray flashes could not be influenced by strong emission lines as observed in the X-ray flash of YZ Ret. In what follows, we regard that the first selection principle is the X-ray detection period, which is not directly influenced by the ambiguity of blackbody fit. Then, the second principle is both the luminosity and temperature to avoid the ambiguity coming from the blackbody fit. Thus, we selected A6 in NGC 3379.

Figure 4 shows the X-ray light curves, already shown in Figure 3(b) and (d), but we add the temporal variation of the photospheric temperature (dotted lines). The blackbody temperature of A6, $kT_{\text{ph}} = 90$ eV, is shown in the upper portion of each panel by the horizontal blue line with a length of 76 days. The X-ray luminosity of A6, $L_X = 1.12 \times 10^{38} \text{ erg s}^{-1}$, is indicated by the horizontal blue line in the lower portion of the same panel. We temporarily set epoch 2 at the first positive detection (around day 4), correspondingly set epoch 3 at the second detection, and epoch 4 at the no detection.

The $1.35 M_{\odot}$ WD model with the mass accretion rate of $\dot{M}_{\text{acc}} = 7.5 \times 10^{-7} M_{\odot} \text{ yr}^{-1}$ is consistent with the observation of A6. On the other hand, $1.2 M_{\odot}$ WD models show much lower X-ray luminosities and lower temperatures, although the flash duration lasts longer. In this way, if we have more frequent observation, we can limit the range of the WD mass and mass accretion rate.

Next, we examine the possibility of A6 in NGC 3379 to be the SSS phase of a helium nova. Similar to hydrogen novae (Kato et al. 2022a, 2024), helium novae also show a much longer SSS phase than those of X-ray flashes. Figure 5 shows the SSS light curve of the $1.35 M_{\odot}$ model with $\dot{M}_{\text{acc}} = 7.5 \times 10^{-7} M_{\odot} \text{ yr}^{-1}$; the SSS phase hardly depends on the mass accretion rate. The X-ray light curve shows a gradual decline over several hundred days. Epoch 1 (nondetection) is far left outside of this figure, which is 1805 days before epoch 2. Early no detection can be attributed to the dust blackout, which should have ended before epoch 2. The gradual decline of the X-ray light curve is inconsistent with nondetection at epoch 4.

The $1.2 M_{\odot}$ models show more gradual decline in the SSS phase over > 3000 days and does not satisfy the observational constrain. Thus, it is unlikely that A6 is in the SSS phase of a helium nova.

Brassington et al. (2012) classified the X-ray source A6 in NGC 3379 to be a classical nova that is in the SSS

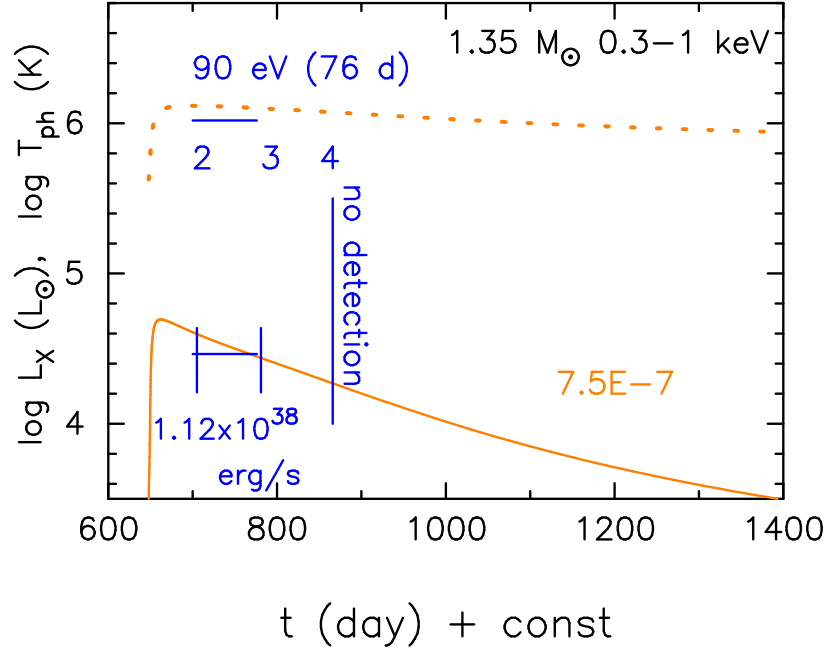


Figure 5. X-ray (0.3 - 1 keV) light curve during the SSS phase of the $1.35 M_{\odot}$ WD with the mass accretion rate of $\dot{M}_{\text{acc}} = 7.5 \times 10^{-7} M_{\odot} \text{ yr}^{-1}$.

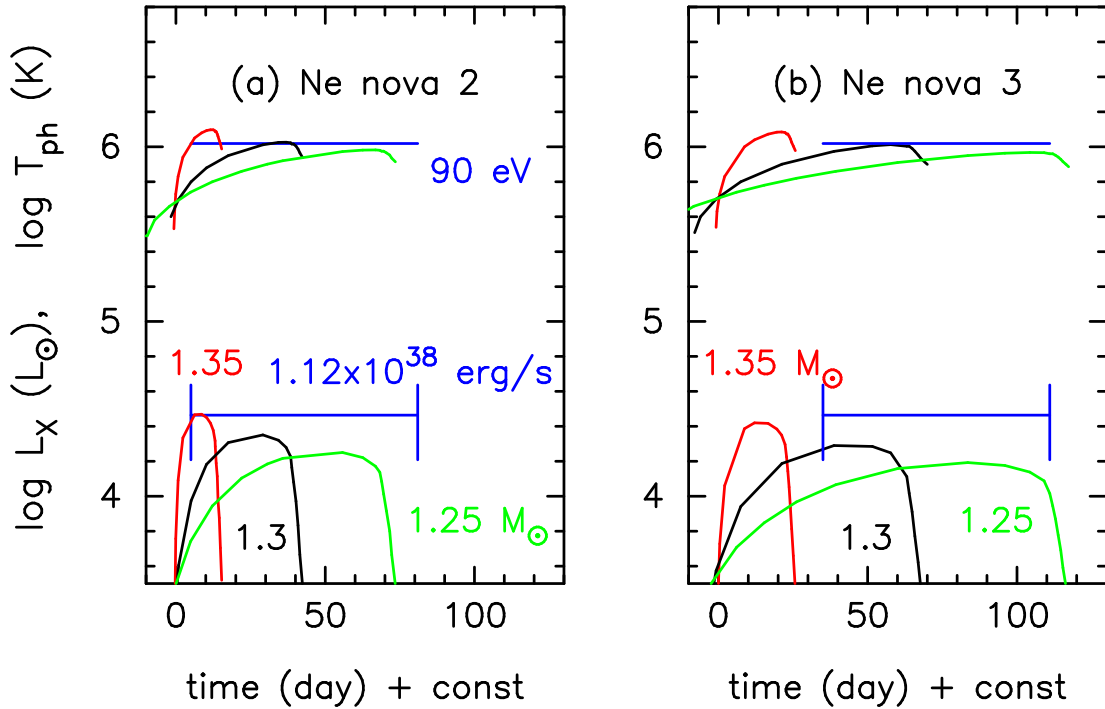


Figure 6. Same as Figure 4, but for the hydrogen-burning SSS phase (0.3 - 1 keV) of classical novae. Each WD mass is attached beside each line; $1.25 M_{\odot}$ (green line), $1.3 M_{\odot}$ (black line), and $1.35 M_{\odot}$ (red line). The chemical composition is assumed to be (a) Ne nova 2, and (b) Ne nova 3 (see the main text). These nova solutions are taken from [Hachisu & Kato \(2016\)](#).

phase. We thus compare the SSS light curves of classical novae with the A6 observation. Figure 6 shows the X-ray light curve (0.3 - 1.0 keV) and temperature evolution of classical nova models of 1.25, 1.3, and 1.35 M_{\odot} WDs with the chemical compositions of the envelope, Neon nova 2 ($X, Y, X_{\text{O}}, X_{\text{Ne}}, Z$) = (0.55, 0.30, 0.10, 0.03, 0.02), and Neon nova 3 (0.65, 0.27, 0.03, 0.03, 0.02), which are taken from Hachisu & Kato (2016). A nova on a more massive WD evolves faster, and the duration of the SSS phase is shorter than 76 days for all the models of Ne nova 2 and 1.35 and 1.3 M_{\odot} WD models for Ne nova 3. Most of the X-ray photons are emitted below 1.0 keV, then the X-ray light curves hardly change even if we adopt a higher upper limit of 8.3 keV corresponding to the Chandra observation. Thus, five of six models are inconsistent with the Chandra observation of A6, although the WD temperature is consistent with the 90 eV. Only the 1.25 M_{\odot} WD (Ne nova 3 composition) shows a longer duration. Its flux is smaller than the luminosity of $L_{\text{X}} = 1.12 \times 10^{38}$ erg s $^{-1}$. We may find a barely consistent model with the lower one σ limit between 1.25 M_{\odot} and 1.3 M_{\odot} of Ne nova 3 or other composition. However, to find a fine tuning model is not our aim of the present work.

Henze et al. (2011, 2014) presented statistical relation between the blackbody temperature kT and the X-ray turnoff time t_{off} of M31 classical novae. Here, the X-ray turnoff time is the time of the SSS phase since the optical outburst, including the optical bright phase.

The value of $t_{\text{off}} \gg 76$ days with 90 eV is outlier of this statistical relation. This suggest that A6 is unlikely to be the SSS phase of a classical nova.

X-ray flashes in hydrogen novae are as short as several days or less (Kato et al. 2016, 2022a,b) and, therefore, are excluded as the explanation of A6. From these comparisons, the supersoft X-ray transient A6 in NGC 3379 is a candidate of an X-ray flash of a helium nova on a $\sim 1.35 M_{\odot}$ WD, although we cannot completely exclude a possibility of the SSS phase of a classical nova.

4. CONCLUDING REMARKS

We have presented theoretical light curves of X-ray flashes for helium novae and found a candidate object of a helium-burning X-ray flash in the literature on extragalactic X-ray surveys. The X-ray flashes last much longer than those of classical novae, i.e., of hydrogen burnings. Such a long duration together with a high X-ray luminosity tells us that X-ray flashes of helium novae are probably detectable. Once an X-ray flash is detected in a helium nova, we can coordinate multiwavelength observations in the following optical rising phase toward maximum. Because a later SSS phase may not be detectable due to a thick dust blackout, the X-ray flash is a valuable tool for us to study helium novae with X-rays.

We are grateful to the anonymous referees for useful comments, which improved the manuscript.

REFERENCES

- Ablimit, I. 2022, MNRAS, 509, 6061, [doi10.1093/mnras/stab3060](https://doi.org/10.1093/mnras/stab3060)
- Ashok, N.M., & Banerjee, D.P.K. 2003, A&A, 409, 1007, <https://doi.org/10.1051/0004-6361:20031160>
- Banerjee, D.P.K., Evans, A., Woodward, C.E., et al. 2003, ApJL, 952, L26, <https://doi.org/10.3847/2041-8213/acdf56>
- Brassington, N.J., Fabbiano, G., Kim, D.-W., et al. 2008, ApJS, 179, 142, <https://doi.org/10.1086/591527>
- Brassington, N.J., Fabbiano, G., Zezas, A., et al. 2012, ApJ, 755, 162, <https://doi.org/10.1088/0004-637X/755/2/162>
- Brooks, J., Bildsten, L., Schwab, J., & Paxton, B. 2016, ApJ, 821, 28, <https://doi.org/10.3847/0004-637X/821/1/28>
- Cassisi, S., Iben, I., Jr., & Tornambé, A. 1998 ApJ, 496, 376, <https://doi.org/10.1086/305381>
- Cui, X., Meng, X.-C., Han, Z.-W. 2018, Research in Astronomy and Astrophysics, 18, 58, <https://doi.org/10.1088/1674-4527/18/5/58>
- Denissenkov, P. A., Herwig, F., Bildsten, L., & Paxton, B. 2013, ApJ, 762, 8, <https://doi.org/10.1088/0004-637X/762/1/8>
- Evans, P. A., Beardmore, A. P., Page, K. L., et al. 2009, MNRAS, 397, 1177, <https://doi.org/10.1111/j.1365-2966.2009.14913.x>
- Greiner, J., et al., 2023, Nature, 615, 605, <https://doi.org/10.1038/s41586-023-05714-4>
- Hachisu, I., & Kato, M. 2010, ApJ, 709, 680, <https://doi.org/10.1088/0004-637X/709/2/680>
- Hachisu, I., & Kato, M. 2016, ApJ, 816, 26, <https://doi.org/10.3847/0004-637X/816/1/26>
- Hachisu, I., & Kato, M. 2022, ApJ, 939, 1, <https://doi.org/10.3847/1538-4357/ac9475>
- Hachisu, I., & Kato, M. 2023, ApJ, 953, 78, <https://doi.org/10.3847/1538-4357/acdfd3>
- Henze, M., Pietsch, W., Habert, F., et al. 2014, A&A, 563, A2, <https://doi.org/10.1051/0004-6361/201322426>

- Henze, M., Pietsch, W., Haberl, F., et al. 2011, *A&A*, 533, A52, <https://doi.org/10.1051/0004-6361/201015887>
- Iben, I. Jr. & Tutukov, A. V. 1989, *ApJ*, 342, 430, <https://doi.org/10.1086/167603>
- Iben, I. Jr. & Tutukov, A. V. 1994, *ApJ*, 431, 264, <https://doi.org/10.1086/174484>
- Idan, I., Shaviv, N. J., & Shaviv, G. 2013, *MNRAS*, 433, 2884, <https://doi.org/10.1093/mnras/stt908>
- Iijima, T. & Nakanishi, H. 2007, *A&A*, 482, 8651, <https://doi.org/10.1051/0004-6361:20077502>
- Jacobson-Galán, W.V., Foley, R. J., Schwab, J., et al. 2019, *MNRAS*, 487, 2538, <https://doi.org/10.1093/mnras/stz1305>
- Kahabka, P., & van den Heuvel, E.P. 1997, *ARA&A*, 35, 69 <https://doi.org/10.1146/annurev.astro.35.1.69>
- Kato, M., & Hachisu, I., 1994, *ApJ*, 437, 802, <https://doi.org/10.1086/175041>
- Kato, M., & Hachisu, I. 2003, *ApJ*, 598, L107, <https://doi.org/10.1086/380597>
- Kato, M., & Hachisu, I. 2020, *PASJ*, 72, 82, <https://doi.org/10.1093/pasj/psaa071>
- Kato, M., Hachisu, I., Kiyota, S., & Saio, H. 2008, *ApJ*, 684, 1366 <https://doi.org/10.1086/590329>
- Kato, M., Hachisu, I., & Saio, H., 2023, *MNRAS*, 525, L56, <https://doi.org/10.1093/mnras/slاد096>
- Kato, M., Saio, H., & Hachisu, I., 1989, *ApJ*, 340, 509, <https://doi.org/10.1086/167413>
- Kato, M., Saio, H., & Hachisu, I. 2017b, *ApJ*, 844, 143, <https://doi.org/10.3847/1538-4357/aa7c5e>
- Kato, M., Saio, H., & Hachisu, I. 2018, *ApJ*, 863, 125, <https://doi.org/10.3847/1538-4357/aad327>
- Kato, M., Saio, H., & Hachisu, I. 2022a, *PASJ*, 74,1005, <https://doi.org/10.1093/pasj/psac051>
- Kato, M., Saio, H., & Hachisu, I. 2022b, *ApJL*, 935, L15, <https://doi.org/10.3847/2041-8213/ac85cl>
- Kato, M., Saio, H., & Hachisu, I. 2022c, *RNAAS*, 6, 258, <https://doi.org/10.3847/2515-5172/aca8af>
- Kato, M., Saio, H., & Hachisu, I. 2024, *PASJ*, 76, 666, <https://doi.org/10.1093/pasj/psae038>
- Kato, M., Saio, H., Henze, M., et al. 2016, *ApJ*, 830, 40, <https://doi.org/10.3847/0004-637X/830/1/40>
- Kato, T., & Kanatsu, K., 2000, *IAU Circ.* 7552
- Kawai, Y., Saio, H., & Nomoto, K., 1988, *ApJ*, 328, 207, <https://doi.org/10.1086/166282>
- Kemp, A.J., Karakas, A. I., Casey, A. R., et al. 2021, *MNRAS*, 504, 6117, <https://doi.org/10.1093/mnras/stab1160>
- König, O., Wilms, J., Arcodia, R., et al. 2022, *Nature*, 605, 248, <https://doi.org/10.1038/s41586-022-04635-y>
- Kovetz, A. 1998, *ApJ*, 495, 401, <https://doi.org/10.1086/305280>
- Kool, E. C., Johansson, J., Sollerman, J. et al. 2023, *Nature*, 617, 477, <https://doi.org/10.1038/s41586-023-05916-w>
- Krautter, J., Ögelman, H., Starrfield, S., Wichmann, R., & Pfeffermann, E. 1996, *ApJ*, 456, 788, <https://doi.org/10.1086/176697>
- Maguire, K., Magee, M.R., Leloudas, G., et al. 2023, *MNRAS*, 525, 1210, <https://doi.org/10.1093/mnras/stad2316>
- Nomoto, K., Saio, H., Kato, M., & Hachisu, I. 2007, *ApJ*, 663, 1269, <https://doi.org/10.1086/518463>
- Osborne, J.P., Page, K.L., Beardmore, A.P., Bode, M.F., Goad, M.R. et al. *ApJ*, 2011, 727, 124, <https://doi.org/10.1088/0004-637X/727/2/124>
- Page, K.L., Osborne, J.P., Kuin, N.P.M., et al., 2015, *MNRAS*, 454, 3108, <https://doi.org/10.1093/mnras/stv2144>
- Sala, G., & Helnanz, M. 2005, *A&A*, 439, 1061, <https://doi.org/10.1051/0004-6361:20042622>
- Sienkiewicz, R. 1975, *A&A*, 45, 411,
- Sienkiewicz, R. 1980, *A&A*, 85, 295
- Taam, R.,E. 1980, *ApJ*, 237, 142, <https://doi.org/10.1086/157852>
- Wang, B., Li, Y., Ma, X., et al. 2015, *A&A*, 584, 37, <https://doi.org/10.1051/0004-6361/201526569>
- Wang, B., Meng, X., Chen, X., & Han, Z. 2009, *MNRAS*, 395, 847, <https://doi.org/10.1111/j.1365-2966.2009.14545.x>
- Wang, B., Podsiadlowski, P., & Han, Z. 2017, *MNRAS*, 472, 1593, <https://doi.org/10.1093/mnras/stx2192>
- Wolf, W. M., Bildsten, L., Brooks, J., & Paxton, B. 2013a, *ApJ*, 777, 136, <https://doi.org/10.1088/0004-637X/777/2/136>; Erratum 782, 117, <https://doi.org/10.1088/0004-637X/782/2/117>
- Wong, T.L.S., & Schwab, J. 2019, *ApJ*, 878, 100 <https://doi.org/10.3847/1538-4357>
- Yoon, S.-C., Langer, N., & Scheithauer, S. 2004, *A&A*, 425, 217, <https://doi.org/10.1051/0004-6361:20040327>